Predicting Index-Mechanical Properties of Igneous Rock Using Electrical Resistivity Method

İsmail İnce[1]

Abstract

The purpose of this study is to investigate the index-mechanical properties of igneous rocks by using electrical resistivity method. To this end, electrical resistivity, index (P-wave velocity, dry density, and porosity), and uniaxial compressive strength values of 48 different igneous rock samples (plutonic, volcanic, and pyroclastic) were measured in the laboratory. Simple regression analysis was performed between index-mechanical properties compatible with the values of electrical resistivity. A strong exponential correlation was obtained between the electrical resistivity and porosity values of the igneous rock samples used in this study. On the other hand, a strong logarithmic correlation was found between the electrical resistivity values and other index-mechanical properties. The electrical resistivity method can be used as a non-destructive method to assess the engineering properties of rocks where it is hard to get regular-shaped rock samples either from an outcrop or a historical building.

Keywords Electrical resistivity · Index-mechanical properties · Regression analysis · Prediction

1 Introduction

The electrical resistivity method is an easy and economical non-destructive technique in geophysics. Its easily applicability both in the field and laboratory conditions increased its usage in different engineering disciplines (geophysics, geology, mining, geotechnical, hydrology, petroleum, and civil), in recent years. Therefore, it is crucial to find out the relationship between electrical resistivity of rocks and their engineering features. The resistivity of rocks, on the other hand, varies depending on porosity [1–3], pore geometry [4, 5], saturation [4–6], heat [7–11], and pressure [12, 13].

In recent years, many researchers have investigated the relationship between the electrical resistivity and index-mechanical properties of rocks [4, 14–21]. Kate and Sthapak [14] determined a logarithmic relationship between resistivity and uniaxial compressive strength (UCS) from a study carried out on the Himalayan rocks. On the other hand, Matsui et al. [4] stated in a study of different rock units (conglomerate, sandstone, granite, shale, and tuff) that the

electrical resistivity values of rocks decreased as the porosity values of rocks increased. Kahraman et al. [16] and Kahraman and Yeken [17] indicated that there is a linear relationship between strength and resistivity values of magmatic rocks. Kahraman and Alber [15] found a logarithmic relationship among UCS, elastic modulus, and resistivity values in a study conducted on fault breccia and indicated that the resistivity values increase with increasing strength values. Su and Momayez [18], on the other hand, investigated the relationships among index (porosity, water absorption), strength (indirect tensile strength, young modulus), and abrasion (Los Angeles abrasion test) properties and electrical resistivity values using simple regression analysis and stated that resistivity values were susceptible to the index and strength properties of rocks. İnce [19] determined a very high correlation between the porosity, dry density, P-wave velocity, and UCS properties and electrical resistivity values of 12 different pyroclastic rock samples taken from the Cappadocia region. Sertçelik et al. [20] carried out a study to discover the correlation coefficient between porosity and electrical resistivity values on different rock and concrete samples. Renibar and Nasab [21] also found a strong correlation between UCS and electrical resistivity in their study on granitic rocks. Some researchers have numerically

✉ İsmail İnce
  iince@ktun.edu.tr

[1] Department of Geological Engineering, Konya Technical University, Konya 42250, Turkey

Table 1 The location and type of the rock samples

Sample	Location	Color	Rock type	Rock name
1	Sille/Konya	Pink	Volcanic	Dacite*
2	Eskişehir	Dark grey	Volcanic	Andesite*
3	Kulu/Konya	Grey	Volcanic	Andesite*
4	Gölbaşı/Ankara	Light brown	Volcanic	Andesite*
5	Gölbaşı/Ankara	Dark grey	Volcanic	Andesite*
6	Kayseri-1	Pink	Volcanic	Andesite*
7	İscehisar/Afyonkarahisar	Pink	Volcanic	Basalt*
8	Sincan/Ankara	Pink	Volcanic	Andesite*
9	Sivrihisar/Eskişehir	Dark grey	Volcanic	Andesite*
10	Sivrihisar/Eskişehir	Light brown	Volcanic	Andesite*
11	Hisar, Kulu/Konya	Pink	Volcanic	Andesite*
12	Hisar, Kulu/Konya	Light grey	Volcanic	Andesite*
13	Yunus Emre/Manisa	Dark pink	Volcanic	Andesite*
14	Çayırlı/Ankara	Brown	Volcanic	Andesite*
15	Yunt/Manisa	Pink to light brown	Volcanic	Andesite*
16	İnsuyu/Kayseri	Dark grey	Volcanic	Andesite*
17	Seydişehir/Konya	Grey	Volcanic	Andesite*
18	Erzurum	Grey	Volcanic	Andesite*
19	Gölbaşı/Ankara	Grey	Volcanic	Andesite*
20	Erkilet/Kayseri	Black	Volcanic	Basalt*
21	Yaylak/Aksaray	Grey	Plutonic	Granite*
22	Kaman/Kırşehir	Grey-light rose	Plutonic	Granite*
23	Bergama/İzmir	Grey	Plutonic	Granite*
24	Ulaş/Kırıkkale	Dark grey	Plutonic	Granite*
25	Kırıkkale	Light grey	Plutonic	Granite*
26	Demirciler/Aksaray	Dark lilac	Pyroclastic	Vitric tuff**
27	Selime/Aksaray	Grayish	Pyroclastic	Vitric tuff**
28	Gümüşler/Niğde	Light pink	Pyroclastic	Vitric tuff**
29	Koçcağız/Kayseri	Yellow	Pyroclastic	Vitric tuff**
30	Kuruköprü/Kayseri	Grayish	Pyroclastic	Vitric tuff**
31	Emmiler/Kayseri	Brownish	Pyroclastic	Vitric tuff**
32	Tomarza/Kayseri	Black	Pyroclastic	Vitric tuff**
33	Karayazı/Nevşehir	White	Pyroclastic	Vitric tuff**
34	Karayazı/Nevşehir	Light yellow	Pyroclastic	Vitric tuff**
35	Karayazı/Nevşehir	Cherry	Pyroclastic	Vitric tuff**
36	Kayseri-2	Grey-1	Pyroclastic	Vitric tuff**
37	Mimarsınan/Kayseri	Grey	Pyroclastic	Vitric tuff**
38	Turanlar/Kayseri	Grey	Pyroclastic	Vitric tuff**
39	Gökyurt/Konya	Light grey	Pyroclastic	Crystal tuff**
40	Kayseri-3	Grey-2	Pyroclastic	Vitric tuff**
41	Kayseri-4	Grey-3	Pyroclastic	Vitric tuff**
42	Aksaray	Light grey	Pyroclastic	Vitric tuff**
43	Karayazı/Nevşehir	Purple	Pyroclastic	Vitric tuff**
44	Karayazı/Nevşehir	Light pink	Pyroclastic	Vitric tuff**
45	Karayazı/Nevşehir	Yellow	Pyroclastic	Crystal tuff**
46	Kızılören/Konya	White–pink spotted	Pyroclastic	Vitric tuff**
47	Ahlat/Bitlis	Brown	Pyroclastic	Vitric tuff**
48	Ardıçlı/Konya	Grey	Pyroclastic	Crystal tuff**

*Rock names given according to Streickeisen [27], **Rock names given according to Schmid [28]

investigated the damage effects of rocks by means of electrical resistivity [22–26].

The objective of this study is to determine the index-strength values of 48 igneous rock (plutonic, volcanic, and pyroclastic) samples, by applying electrical resistivity method.

2 Materials and Methods

Forty-eight igneous rock samples collected from the Anatolian region in Turkey were used in this study. The samples locations and rock types are shown in Table 1. The types of the rock samples are plutonic, volcanic, and pyroclastic.

2.1 Experimental Procedure

Nearly uniform rock specimens were collected from the quarries for laboratory tests with dimensions of $20 \times 30 \times 30$ cm. Test specimens were prepared in accordance with the pertinent standards and suggested test methods [29, 30] in order to ascertain their relevant engineering properties. Porosity (n), water absorption by weight (Wa), dry density (ρd), and P-wave velocity (Vp) tests were performed according to ISRM [29] on cylindrical rock samples. Porosity and water absorption by weight values of the rocks were found by applying saturation and caliper procedures [29]. To determine the dry density of the samples, the volume of the rock samples was first calculated by averaging several caliper readings. Then, the dry density of the samples was determined as mass of a unit volume of rock sample. P-wave velocity of the rocks was measured over the samples by direct transmission using PUNDIT, which measures the propagation time of ultrasound pulses with an accuracy of 0.1 µs (Fig. 1a). UCS tests were performed on core samples with a diameter of 54 mm and a length of 110 mm according to ASTM D2938 [30] (Fig. 1b). The loading rate within the limits of 1.0 ± 0.5 MPa/s was applied. UCS tests were run five times for each rock sample, and the average UCS value of each specimen was determined.

Thin sections of the samples were prepared in accordance with TS EN-12407 [31] and examined under an optical microscope from Nikon. Volcanic and plutonic rocks and pyroclastic rocks were classified and named according to the Streckeisen [27]'s and Schmid [28]'s classifications, respectively (Table 1).

2.1.1 Electrical Resistivity Measurements

Measurements of electrical resistivity were carried out on the core specimens having 54-mm diameter and approximately 110-mm length. Both surfaces of the core specimens were made flat and parallel to each other. The specimens were completely saturated with distilled water. The saturation of the samples was checked by measuring the increase in weight. In this case, if there was no extra weight increase in the samples, they were considered to be fully saturated. The mechanism depicted in Fig. 2 was used in resistivity measurements. Circular copper electrodes which had the equal diameter same as the specimens were used in the experiments. Twelve-voltage direct current (DC) was exerted across the rock specimen. After exerting the voltage at room temperature, its reaction was measured.

Utilizing the geometry and the resistance of the specimens, amount of electrical resistivity were computed from the equation below:
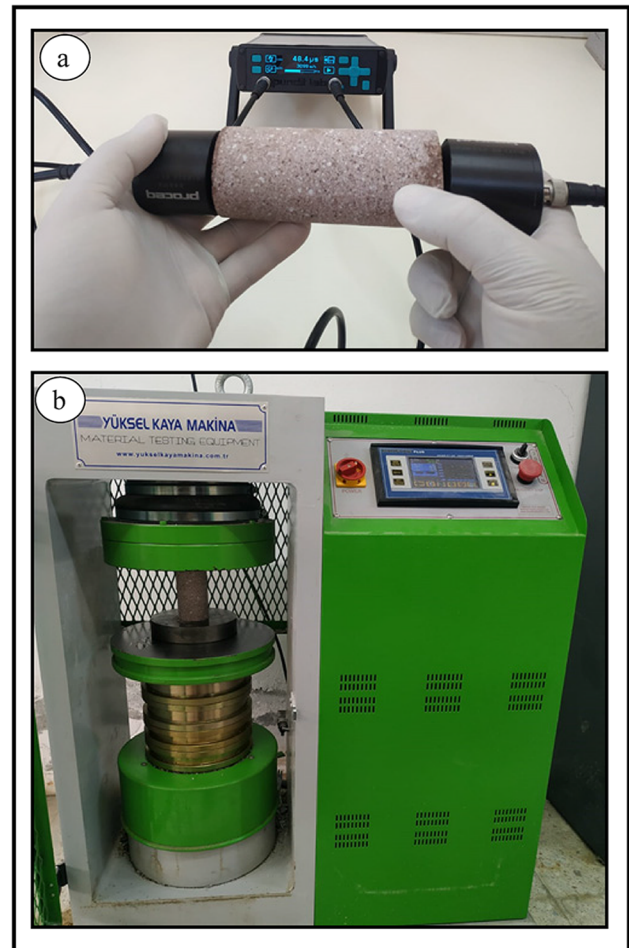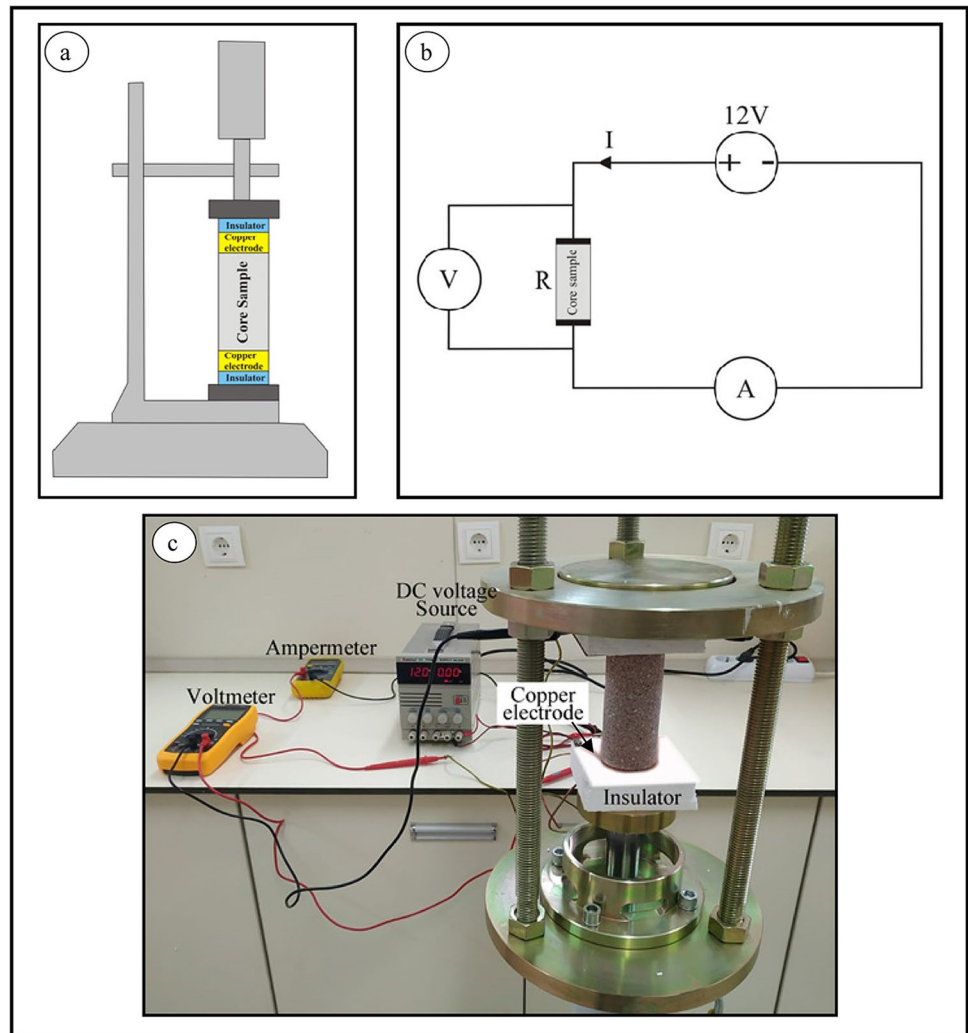
$$\rho = \frac{RA}{L} \tag{1}$$

Fig. 1 Measurement of some index-mechanical properties: **a** P-wave velocity, **b** uniaxial compressive strength

Fig. 2 The device used in measurements of resistivity: **a** schematic diagram, **b** electronic circuit design, **c** resistivity measurement system (V, voltmeter; A, ampere meter; 12 V, DC voltage source; I, current; R, resistance)

where ρ is the electrical resistivity and R is the resistance. A and L are the cross-section area and the length of rock sample, respectively.

$$R = \frac{V}{I} \tag{2}$$

where R, V, and I are called the resistance, the volt, and the current, respectively.

3 Results and Discussion

The index, the UCS, and the electrical resistivity values of the igneous rocks used in this study are given in Table 2. Statistical analyses of these data are presented in Table 3.

The dry densities of the igneous rocks used in the study vary between 1.23 and 2.68 g/cm³, whereas porosity values vary between 0.86 and 36.83%. According to

dry density classification of the NBG [32], the dry density values of the volcanic and plutonic rocks fall into the high-very high class, whereas pyroclastic rocks fall into the very low class. On the other hand, according to porosity classification of the NBG [32], porosity values of the igneous rocks take place in between low to very high class. The water absorption by weight values of these rocks range between 0.32 and 28.27%. The highest P-wave velocity was measured in the basalt sample number 20 as 5.38 km/s, while the lowest P-wave velocity was measured in the pyroclastic sample number 39 as 0.89 km/s. The UCS test results of the rock specimens used in this study vary between 6.87 and 179.39 MPa. According to the ISRM [33] classification, the UCS values of the volcanic and plutonic rocks are classified as medium to high rock class, whereas the pyroclastic rocks classified as low and low-medium class. The measured resistivity values of the samples used in this study vary between 37.97 and 8997.53 $\Omega m^2/m$. The lowest

Table 2 Some physico-mechanical and electrical resistivity properties of the rock samples (mean value ± standard deviation)

Sample	Test number	ρ_d g/cm³	n %	Wa %	Vp km/s	UCS MPa	ρ Ωm²/m
1	5	2.32 ± 0.03	5.65 ± 0.60	2.41 ± 0.30	3.78 ± 0.05	60.60 ± 5.50	720.44 ± 25.05
2	5	2.38 ± 0.01	4.81 ± 0.21	2.02 ± 0.12	4.91 ± 0.02	78.20 ± 4.12	1476.86 ± 35.40
3	5	2.48 ± 0.02	5.54 ± 0.32	2.24 ± 0.17	4.12 ± 0.06	59.88 ± 3.25	723.18 ± 32.45
4	5	2.36 ± 0.02	7.11 ± 0.37	3.02 ± 0.21	4.82 ± 0.04	67.59 ± 5.10	664.61 ± 23.19
5	5	2.51 ± 0.01	4.37 ± 0.20	1.74 ± 0.12	4.67 ± 0.06	64.94 ± 2.07	615.31 ± 38.48
6	5	2.28 ± 0.03	7.16 ± 0.42	3.14 ± 0.19	3.97 ± 0.02	61.30 ± 3.42	378.00 ± 28.90
7	5	2.25 ± 0.02	8.23 ± 0.17	3.66 ± 0.09	4.25 ± 0.03	63.85 ± 4.18	488.41 ± 57.18
8	5	2.35 ± 0.02	5.16 ± 0.13	2.20 ± 0.0	4.10 ± 0.05	50.68 ± 2.10	313.71 ± 19.78
9	5	2.34 ± 0.03	7.29 ± 0.27	3.12 ± 0.13	4.66 ± 0.02	111.35 ± 6.75	976.40 ± 39.41
10	5	2.34 ± 0.01	6.30 ± 0.24	2.69 ± 0.11	4.76 ± 0.06	71.16 ± 3.45	845.02 ± 28.74
11	5	2.30 ± 0.01	8.68 ± 0.19	3.77 ± 0.09	3.90 ± 0.05	83.63 ± 5.12	554.86 ± 25.13
12	5	2.34 ± 0.02	8.37 ± 0.28	3.58 ± 0.13	3.95 ± 0.04	83.11 ± 2.16	976.40 ± 71.12
13	5	2.34 ± 0.04	6.80 ± 0.11	2.90 ± 0.06	4.40 ± 0.02	91.68 ± 9.23	845.02 ± 41.20
14	5	2.22 ± 0.03	12.30 ± 0.19	5.53 ± 0.10	3.57 ± 0.07	48.13 ± 6.02	554.86 ± 30.98
15	5	2.43 ± 0.02	3.46 ± 0.12	1.43 ± 0.12	4.65 ± 0.06	89.60 ± 3.94	457.89 ± 18.74
16	5	2.36 ± 0.01	6.87 ± 0.31	2.91 ± 0.17	2.14 ± 0.02	78.60 ± 5.34	1250.62 ± 89.38
17	5	2.38 ± 0.01	7.43 ± 0.41	3.13 ± 0.20	3.42 ± 0.03	68.97 ± 3.78	441.46 ± 43.21
18	5	2.48 ± 0.02	1.64 ± 0.18	0.66 ± 0.10	4.72 ± 0.03	179.39 ± 10.03	2884.18 ± 100.12
19	5	2.46 ± 0.02	6.04 ± 0.26	2.46 ± 0.14	4.36 ± 0.03	100.47 ± 9.71	691.05 ± 56.43
20	5	2.61 ± 0.06	3.49 ± 1.08	1.34 ± 0.47	5.38 ± 0.14	112.79 ± 7.79	1981.50 ± 28.74
21	5	2.62 ± 0.01	1.02 ± 0.08	0.39 ± 0.03	4.42 ± 0.04	141.56 ± 12.20	8997.53 ± 49.32
22	5	2.68 ± 0.01	0.86 ± 0.06	0.32 ± 0.04	4.34 ± 0.38	125.74 ± 8.50	2077.55 ± 64.23
23	5	2.66 ± 0.03	1.14 ± 0.13	0.43 ± 0.07	4.71 ± 0.06	176.00 ± 7.09	2805.83 ± 81.42
24	5	2.66 ± 0.02	1.23 ± 0.19	0.46 ± 0.11	4.81 ± 0.10	106.40 ± 5.13	3443.50 ± 43.38
25	5	2.63 ± 0.01	1.13 ± 0.21	0.43 ± 0.09	4.70 ± 0.05	96.25 ± 4.39	5180.19 ± 86.23
26	5	1.75 ± 0.03	23.89 ± 0.49	13.69 ± 0.58	2.95 ± 0.02	48.63 ± 2.50	179.03 ± 20.18
27	5	1.54 ± 0.05	24.81 ± 0.49	16.13 ± 0.39	2.30 ± 0.23	10.55 ± 0.60	181.23 ± 31.28
28	5	1.30 ± 0.01	36.83 ± 0.68	28.23 ± 0.69	2.02 ± 0.02	7.57 ± 0.65	37.97 ± 4.54
29	5	1.63 ± 0.04	25.57 ± 1.80	15.75 ± 1.53	2.58 ± 0.06	31.57 ± 1.81	129.91 ± 8.51
30	5	1.78 ± 0.01	19.53 ± 0.58	10.96 ± 0.35	2.28 ± 0.01	48.38 ± 9.84	227.88 ± 12.05
31	5	1.82 ± 0.02	26.21 ± 0.61	14.44 ± 0.52	2.69 ± 0.08	36.64 ± 5.46	118.08 ± 7.68
32	5	1.42 ± 0.02	33.05 ± 0.56	23.30 ± 0.64	2.90 ± 0.05	27.27 ± 1.69	242.00 ± 5.42
33	5	1.75 ± 0.06	21.09 ± 1.85	12.07 ± 1.45	2.45 ± 0.05	16.86 ± 0.81	111.49 ± 4
34	5	1.54 ± 0.02	28.45 ± 0.69	18.45 ± 0.48	2.49 ± 0.06	24.51 ± 1.28	242.00 ± 6.10
35	5	1.66 ± 0.02	30.76 ± 0.45	18.49 ± 0.41	2.19 ± 0.05	15.68 ± 1.68	53.54 ± 1.74
36	5	1.94 ± 0.02	14.84 ± 0.51	7.64 ± 0.26	2.64 ± 0.07	48.76 ± 7.19	306.10 ± 12.51
37	5	1.82 ± 0.03	20.16 ± 0.32	11.08 ± 0.16	2.27 ± 0.02	32.00 ± 3.71	369.02 ± 20.43
38	5	2.03 ± 0.01	15.32 ± 0.48	7.54 ± 0.24	2.65 ± 0.04	59.71 ± 2.16	504.18 ± 40.13
39	5	1.74 ± 0.02	26.49 ± 0.61	15.27 ± 0.31	0.89 ± 0.01	12.10 ± 1.13	127.15 ± 8.87
40	5	2.01 ± 0.01	12.67 ± 0.51	6.30 ± 0.25	2.57 ± 0.05	42.13 ± 4.02	399.13 ± 35.98
41	5	1.80 ± 0.03	21.33 ± 0.43	12.11 ± 0.22	2.73 ± 0.04	28.00 ± 1.10	307.51 ± 12.85
42	5	1.84 ± 0.02	19.11 ± 0.75	10.35 ± 0.37	2.95 ± 0.06	39.62 ± 2.12	205.40 ± 5.78
43	5	1.44 ± 0.01	31.31 ± 0.86	21.68 ± 0.42	2.13 ± 0.07	6.87 ± 0.95	102.53 ± 2.10
44	5	1.56 ± 0.02	29.25 ± 0.74	18.73 ± 0.38	2.15 ± 0.03	8.76 ± 1.06	99.72 ± 2.50
45	5	1.64 ± 0.02	28.68 ± 0.52	17.48 ± 0.21	2.52 ± 0.02	13.57 ± 0.85	130.40 ± 3.45
46	5	1.23 ± 0.01	34.89 ± 0.43	28.27 ± 0.19	2.04 ± 0.05	11.02 ± 1.45	75.49 ± 2.01
47	5	1.49 ± 0.02	34.29 ± 0.35	23.04 ± 0.21	2.57 ± 0.04	9.52 ± 0.45	151.28 ± 3.90
48	5	1.86 ± 0.03	16.83 ± 0.21	9.07 ± 0.11	1.56 ± 0.02	13.78 ± 0.73	74.00 ± 1.98

ρ_d dry density, *n* porosity, *Wa* water absorption by weight, *Vp* P-wave velocity, *UCS* uniaxial compressive strength, ρ electrical resistivity

Table 3 Descriptive statistics of data used in the analysis

Variables	Data	Mean	Std. deviation	Variance	Minimum	Maximum
ρ_d- g/cm³	48	2.07	0.42	0.18	1.23	2.68
n -%	48	14.74	11.22	125.92	0.86	36.83
Aw -%	48	8.67	8.06	6504	0.32	28.27
Vp -km/s	48	3.38	1.12	1.26	0.89	5.38
UCS -MPa	48	59.70	42.78	1829.97	6.87	179.39
ρ- Ωm²/m	48	931.65	1560.74	2,435,906.15	37.97	8997.53

ρ_d dry density, *n* porosity, *Wa* water absorption by weight, *Vp* P-wave velocity, *UCS* uniaxial compressive strength,*ρ* electrical resistivity

Table 4 Correlation between electrical resistivity vs. index and strength values of the samples

Rock properties	Equation	r
n	$n = 1173 * \rho^{-0.794}$	0.91
ρ_d	$\rho_d = 0.3ln(\rho) + 0.256$	0.88
Vp	$Vp = 0.7108ln(\rho) - 0.901$	0.80
UCS	$UCS = 30.899ln(\rho) - 127.13$	0.89

ρ_d dry density, *n* porosity, *Vp* P-wave velocity, *UCS* uniaxial compressive strength,*ρ* electrical resistivity

resistivity values were measured in the pyroclastic rocks whereas the highest resistivity values were measured in plutonic rocks.

The relationship among the index, the UCS, and the electrical resistivity was investigated using the simple regression analysis. The accuracy of the derived equations was controlled by means of *t* and *F* test. If the computed *t* and *F* values are greater than those which were arranged, null hypothesis is dismissed. This result shows that *r* value is important. If the calculated *t* and *F* values are less than
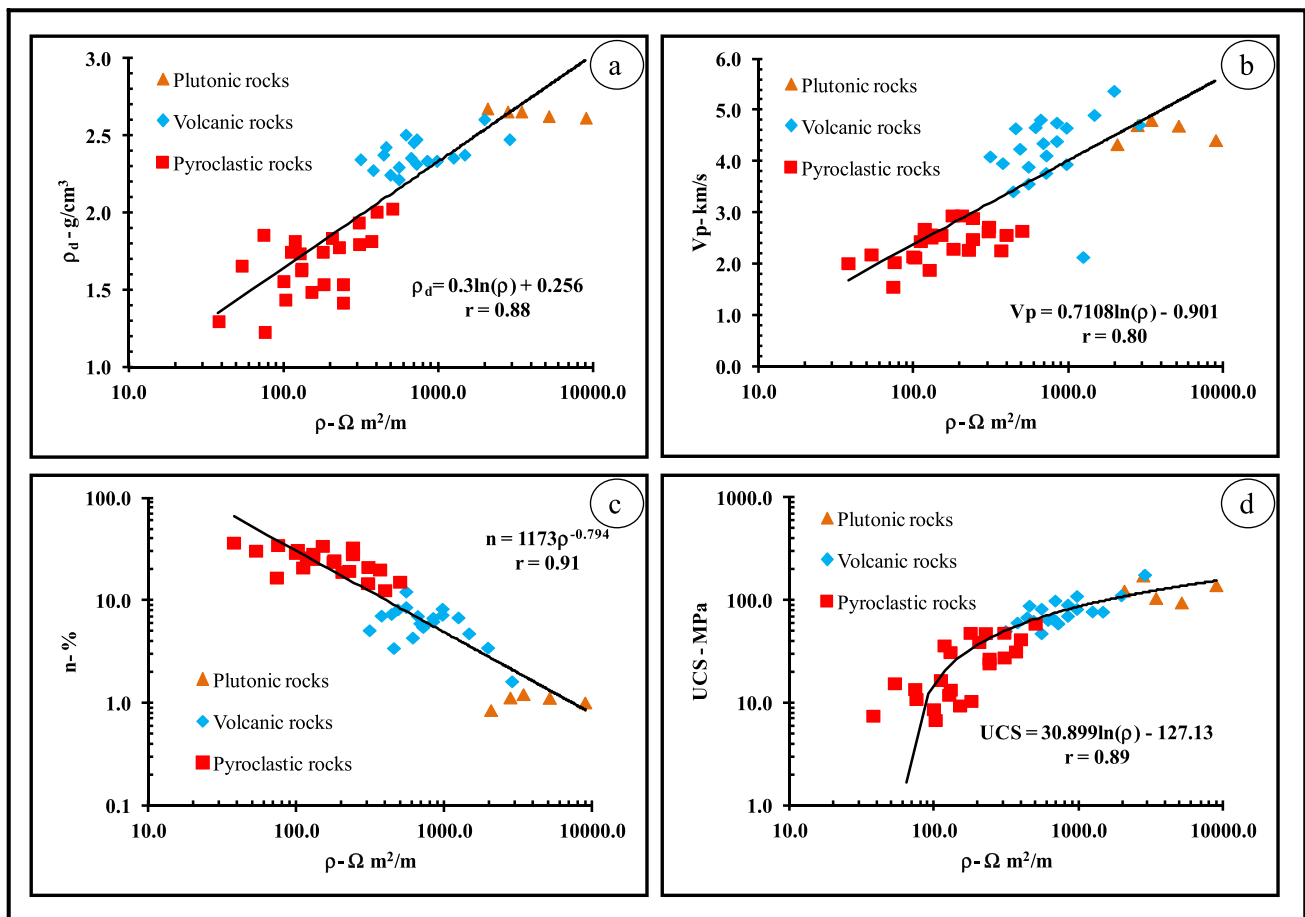

Fig. 3 Correlation between electrical resistivity: **a** dry density, **b** P-wave velocity, **c** porosity, **d** uniaxial compressive strength

Table 5 The variance analysis of the models

Rock properties	r	t test	F test	$p < 0.05$
n	0.91	− 14.961	223.820	0.000
ρ_d	0.88	12.457	155.186	0.000
V_p	0.80	8.907	79.335	0.000
UCS	0.89	13.018	96.166	0.000

ρ_d dry density, n porosity, Vp P-wave velocity, UCS uniaxial compressive strength

those of the arranged values, null hypothesis is not dismissed and r value is not significant. The computed values are bigger than the arranged t and F values showing that the models in the study are accurate. For the reliability of the derived equations for 5% significance level ($\alpha = 0.05$), p value is required to be less than 0.05. In the determination of the best equation within the equations providing this requirement, the equation having the biggest correlation coefficient (r) value was taken into account. The equations derived are given in Table 4. The graphs created for them are presented in Fig. 3. The analyses of variance for the

confirmation of equations were implemented and the outcomes are presented in Table 5. In this experimental study, a 95% significance level was preferred. The developed statistical models demonstrated that they could be used reliably in the estimation of strength values for a significance level of 5%.

There is a logarithmic correlation between density and electrical resistivity values having correlation coefficient (r) value of 0.88 (Fig. 3a). The resistivity values of rocks increase with increasing density values. The correlation coefficient value (r) was found to be 0.80 in the relationship between P-wave velocity and electrical resistivity values (Fig. 3b). When the low value of r compared to other properties was examined, it was found that some points deviated from the matched curve. This situation was connected with the rock properties (e.g., grain size and porosity) influencing the P-wave velocity, as stated by Fener [34]. A power relationship was determined between porosity and electrical resistivity values. The r value of this relationship was 0.91 (Fig. 3c). The porosity values of the rocks increase with decreasing resistivity values. There was a logarithmic
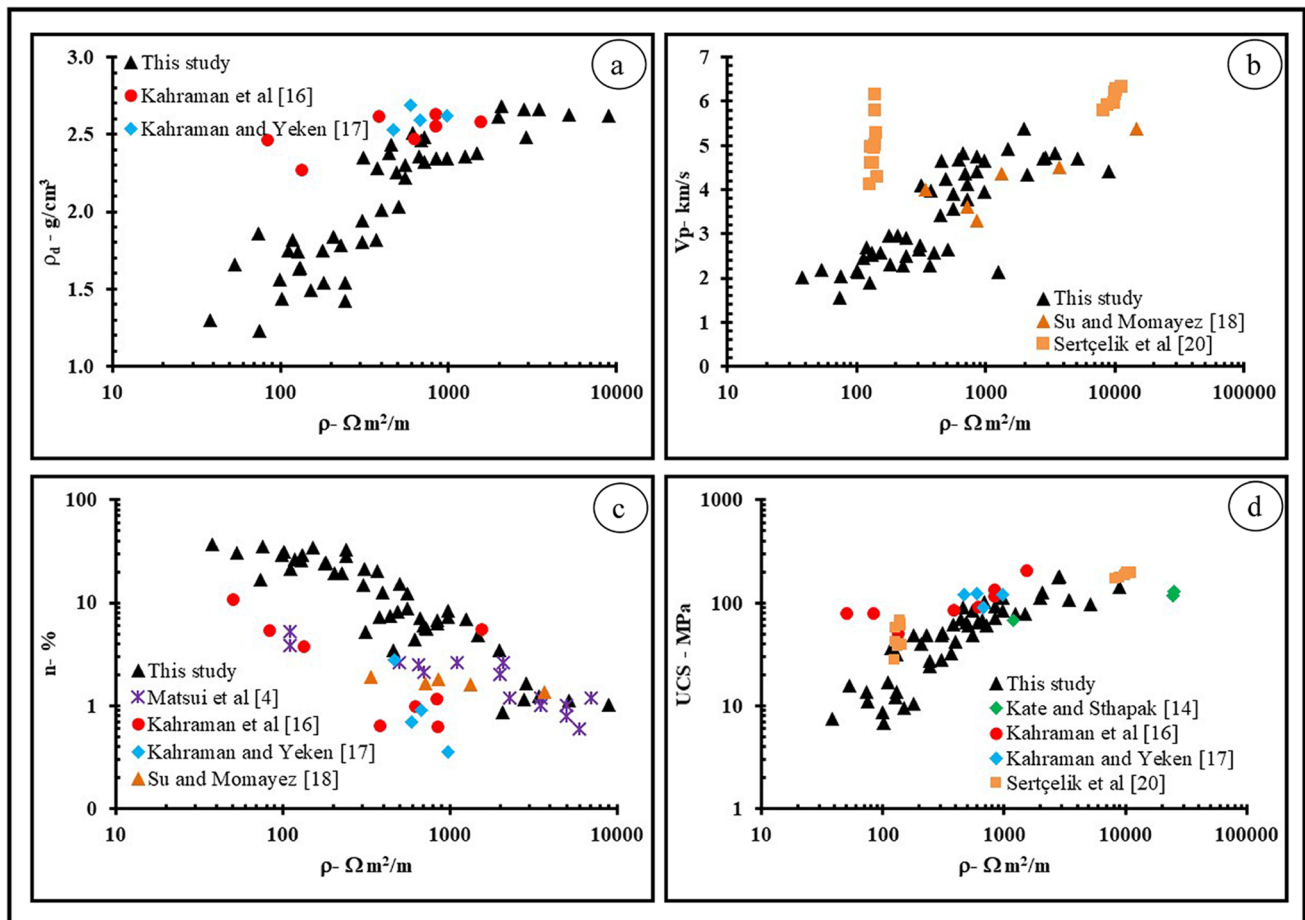

Fig. 4 The comparison of data obtained from this study with those of other studies: **a** dry density, **b** P-wave velocity, **c** porosity, **d** uniaxial compressive strength

relationship between UCS and the resistivity value, and the *r* value was 0.89. The UCS values of the rocks also increase with increasing resistivity values (Fig. 3d).

Figure 4 shows the comparison between resistivity and index-mechanical (ρ_d, Vp, n, UCS) data of magmatic rocks from previous studies and this study. This figure indicates that index-mechanical data range in previous studies is quite limited. However, the data range of index-mechanical properties of rocks used in this study is quite wide. This increases the usability and reliability of the equations developed in this study.

4 Conclusions

In this study, the relationship between the index-mechanical properties and electrical resistivity was investigated on 48 different rock samples representing 3 different rock types (plutonic, volcanic, and pyroclastic). Electrical resistivity is influenced by the physico-mechanical properties of igneous rocks such as porosity, dry density, and index-strength. The general conclusions achieved in this study can be summarized as follows:

- The best connection between electrical resistivity and porosity was found in the power function. On the other hand, the best connection between electrical resistivity and the other properties was defined in the logarithmical function. A very high correlation was identified between electrical resistivity values and index-strength values.
- The electrical resistivity of rocks increases with increasing the dry density. However, the electrical resistivity of rocks decreases with increasing porosity. The resistivity of rocks increases with increasing UCS value.

Consequently, measurement of electrical resistivity is a relatively fast and cost-effective non-destructive method for determining the engineering properties of rocks. Therefore, this method can be useful in determining mechanical and index properties of rocks where it is difficult and impossible to collect samples either from outcrop or from historical and cultural structures without damaging them.

Declarations

Conflict of Interest The author declares no competing interests.

References

1. Boyce RE (1968) Electrical resistivity of modern marine sediments from the Bering Sea. J Geophys Res 73:4759–4766. https://doi.org/10.1029/JB073i014p04759
2. Kermabon A, Gehin C, Blavier P (1969) A deep-sea electrical resistivity probe for measuring porosity and density of unconsolidated sediments. Geophys 34:554–571. https://doi.org/10.1190/1.1440031
3. Keller GV (1974) Engineering applications of electrical geophysical methods: Proceedings of Conference on Subsurface Exploration for Underground Excavation and Heavy Construction, Henniker, New Hampshire, pp 128–143
4. Matsui T, Park SG, Park MK, Matsuura S (2000) Relationship between electrical resistivity and physical properties of rocks. ISRM International Symposium, Melbourne, Australia, pp 19–24
5. Khairy H, Harith ZZT (2011) Influence of pore geometry, pressure and partial water saturation to electrical properties of reservoir rock: measurement and model development. J Petrol Sci Eng 78:687–704. https://doi.org/10.1016/j.petrol.2011.07.018
6. Rahman T, Lebedev M, Zhang Y, Barifcani A, Iglauer S (2017) Influence of rock microstructure on its electrical properties: an analysis using x-ray microcomputed tomography. Energy Procedia 114:5023–5031. https://doi.org/10.1016/j.egypro.2017.03.1651
7. Llera F, Sato M, Nakatsuka K, Yokoyama H (1990) Temperature dependence of the electrical resistivity of water-saturated rocks. Geophys 55(5):576–585. https://doi.org/10.1190/1.1442869
8. Mostafa M, Afify N, Gaber A, Abozid E (2003) Electrical resistivity of some basalt and granite samples from Egypt. Egyption J Solids 26:25–32
9. Zhang W, Sun Q, Zhu S, Hao S (2017) The effect of thermal damage on the electrical resistivity of sandstone. J Geophys Eng 14:255–261. https://doi.org/10.1088/1742-2140/aa5a22
10. Zhang W, Sun Q, Hao SQ, Yang L (2016) Experimental study of the effect of thermal damage on resistivity and mechanical properties of sandstone. Acta Geodyn Geomater 13(2):185–192. https://doi.org/10.13168/AGG.2015.0056
11. Lü C, Sun Q (2018) Electrical resistivity evolution and brittle failure of sandstone after exposure to different temperatures. Rock Mech Rock Eng 51(2):639–645. https://doi.org/10.1007/s00603-017-1351-7
12. Gokhale CS (1999) Studies on strength, deformation and electrical resistivity behaviour of certain sedimentary rocks. PhD Thesis, Indian Institute of Technology.
13. Sun Q, Zhu S, Xue L (2015) Electrical resistivity variation in uniaxial rock compression. Arabian J Geosci 8:1869–1880. https://doi.org/10.1007/s12517-014-1381-3
14. Kate J, Sthapak A (1995) Engineering behaviour of certain Himalayan rocks. The 35th US Symposium on Rock Mechanics (USRMS), Nevada, pp 783–788
15. Kahraman S, Alber M (2006) Predicting the physico-mechanical properties of rocks from electrical impedance spectroscopy measurements. Int J Rock Mech Min Sci 43:543–553. https://doi.org/10.1016/j.ijrmms.2005.09.013
16. Kahraman S, Ogretici E, Fener M, Yeken T (2006) Predicting the physico-mechanical properties of igneous rocks from electrical resistivity measurements. EUROCK, Belgium, pp 557–560
17. Kahraman S, Yeken T (2010) Electrical resistivity measurement to predict uniaxial compressive and tensile strength of igneous rocks. Bull Mater Sci 33:731–735. https://doi.org/10.1007/s12034-011-0137-x
18. Su O, Momayez M (2017) Indirect estimation of electrical resistivity by abrasion and physico-mechanical properties of rocks. J

Appl Geophys 143:23–30. https://doi.org/10.1016/j.jappgeo.2017.05.006

19. İnce İ (2018) Determination of index-strength properties of pyroclastic rocks by electrical resistivity method. OHU J Eng Sci 7(2):772–780. https://doi.org/10.28948/ngumuh.444789

20. Sertçelik İ, Kurtuluş C, Sertçelik F, Pekşen E, Aşçı M (2018) Investigation into relations between physical and electrical properties of rocks and concretes. J Geophys Eng 15(1):142–152. https://doi.org/10.1088/1742-2140/aa87ca

21. Renibar S, Nasab SK (2019) Determination of uniaxial compressive strength of granite rock samples using electrical resistivity measurement: NDT. Conference Proceedings, EAGE-GSM 2nd Asia Pacific Meeting on Near Surface Geoscience and Engineering, 2019: 1–5. https://doi.org/10.3997/2214-4609.201900452

22. Wu G, Wang K, Zhao M, Nie Z, Huang Z (2019) Analysis of damage evolution of sandstone under uniaxial loading and unloading conditions based on resistivity characteristics. Adv Civ Eng 2019:9286819. https://doi.org/10.1155/2019/9286819

23. Yin D, Xu Q (2020) Comparison of sandstone damage measurements based on non-destructive testing. Mater 13(22):5154. https://doi.org/10.3390/ma13225154

24. Yin D, Xu Q (2021) Investigating the damage evolution of sandstone using electrical impedance spectroscopy. Int J Rock Mech Min Sci 144:104817. https://doi.org/10.1016/j.ijrmms.2021.104817

25. Wang K, Li X, Huang Z, Zhao M (2021) Experimental study on acoustic emission and resistivity response of sandstone under constant amplitude cyclic loading. Adv Mater Sci Eng 2021:6637200. https://doi.org/10.1155/2021/6637200

26. Wang K, Xia Z, Li HZ, X, (2021) Damage evolution of sandstone under constant-amplitude cyclic loading based on acoustic emission parameters and resistivity. Adv Mater Sci Eng 2021:7057183. https://doi.org/10.1155/2021/7057183

27. Streickeisen A (1979) Classification and nomenclature of volcanic rock lomprophyres, corbanatites and millitic rocks. Geol 7:331–335

28. Schmid R (1981) Descriptive nomenclature and classification of pyroclastic deposits and fragments: recommendations of the international union of geological sciences subcommission on the systematics of igneous rocks. Geol 9:41–43

29. ISRM (2007) The Complete ISRM Suggested Methods for Rock Characterization, Testing and Monitoring: 1974–2006. (in Ulusay R, Hudson J Eds), International Society for Rock Mechanics, Commission on Testing Methods, Ankara, Turkey

30. ASTM D2938 (1986) Standard test method for unconfined compressive strength of intact rock core specimens. Annual book of ASTM standards, American Society for Testing and Materials, West Conshohocken

31. TS EN-12407 (2019) Natural stone test methods - Petrographic examination. Turkish Standards Institution, Ankara

32. NBG (1985) Engineering Geology and Rock Engineering: Norwegian Group of Rock Mechanics. Fornebu, Norway

33. ISRM (1979) Suggested methods for determining the uniaxial compressive strength and deformability of rock materials. Int J Rock Mech Min Sci 16:135–140

34. Fener M (2011) The effect of rock sample dimension on the P-wave velocity. J Nondestr Eval 30:99–105. https://doi.org/10.1007/s10921-011-0095-7

Publisher's Note Springer Nature remains neutral with regard to jurisdictional claims in published maps and institutional affiliations.